Results in Physics 53 (2023) 106983

Contents lists available at ScienceDirect

Results in Physics

journal homepage: www.elsevier.com/locate/rinp

Influence analysis of uncertainty of chemical reaction rate under different reentry heights on the plasma sheath and terahertz transmission characteristics

Wenchong Ouyang [a,c], Chengbiao Ding [c,e], Qi Liu [b,c], Quanming Lu [a,d], Zhengwei Wu [b,c,d,*]

[a] Deep Space Exploration Laboratory, School of Earth and Space Sciences, University of Science and Technology of China, Hefei 230026, China
[b] School of Nuclear Science and Technology, University of Science and Technology of China, Hefei 230026, China
[c] Joint Laboratory of Plasma Application Technology, Institute of Advanced Technology, University of Science and Technology of China, Hefei 230031, China
[d] CAS Key Laboratory of Geospace Environment, University of Science and Technology of China, Hefei 230026, China
[e] Department of Rehabilitation Medicine, The Second Hospital of Anhui Medical University, Hefei 230601, China

ARTICLE INFO

Keywords:
Terahertz wave
Plasma flow
Plasma sheath
Flight parameters
Chemical reaction
Attenuation

ABSTRACT

Plasma sheath prediction of hypersonic vehicle is critical to radio frequency (RF) blackout solutions as well as vehicle design and development. In this paper, an optimized chemical reaction (OCR) model by considering the difference in reaction rate coefficient under different re-entry heights is proposed to obtain more accurate plasma sheath distribution. In the OCR model, the correction coefficient of chemical reaction rate at different heights is obtained by deriving the relationship between vehicle surface temperature and reaction rate. Further, through the coupling with hypersonic plasma flow model and co-simulation with terahertz transmission model, the influence of reaction rate uncertainty on the plasma sheath and terahertz transmission characteristics under different heights is studied. The reaction rate uncertainty has little effect on the collision frequency and sheath thickness, but has a significant effect on the electron density. Numerical simulations and comparisons with flight data validate the electron density prediction accuracy of OCR model was improved by more than 13.1% compared with the traditional chemical reaction (TCR) model, which causes prediction accuracy of signal attenuation at 0.05 THz improves about 25%, and it gradually decreases with the increasing terahertz frequency. The above conclusions are of great significance for the communication attenuation prediction and RF blackout schemes.

Introduction

During the reentry of hypersonic vehicle or spacecraft return capsule, the plasma sheath is formed due to the shock wave effect and chemical non-equilibrium effect caused by ultra-high speed [1–2]. Plasma sheath has a significant impact on the tracking, telemetry and command (TT&C) systems, and in severe cases can produce RF blackout, posing a serious threat to vehicle safety [3–4]. Therefore, accurate plasma sheath distribution is the basis for interaction between electromagnetic (EM) wave, reentry communication prediction, and plasma sheath and proposal of RF blackout mitigation scheme [5]. Although the electronic density and other data were obtained by reentry flight project, the entire plasma sheath distribution could not be obtained, and reentry flight experiment is difficult to carry out due to large resources [6–7].

In recent years, many numerical models by computational fluid dynamics (CFD) method have been developed to investigate the plasma sheath characteristics, and reentry communication schemes is further studied by combining electromagnetic computing models. Kundrapu and Tang *et al* use finite volume method to solve the plasma sheath characteristics of Radio Attenuation Measurement C (RAM C) vehicle under chemical nonequilibrium (7 species chemical model), and the potential feasibility of magnetic window and terahertz communication schemes is verified by finite-difference time-domain (FDTD) and scattering matrix method (SMM) method, respectively [8–12]. Takahashi *et al* have developed flow field model under thermochemical nonequilibrium flow (11 species chemical model and two-temperature model) based on the RG-FaSTAR solver to obtain plasma sheath distribution, and combined with FD2TD method to predict the vehicle reentry communication [13–14]. Li *et al* have proposed a multi-physical coupling model of plasma flow and EM based on the ANSYS fluent

* Corresponding author at: School of Nuclear Science and Technology, University of Science and Technology of China, Hefei 230026, China.
E-mail address: wuzw@ustc.edu.cn (Z. Wu).

https://doi.org/10.1016/j.rinp.2023.106983
Received 9 July 2023; Received in revised form 29 August 2023; Accepted 12 September 2023
Available online 13 September 2023

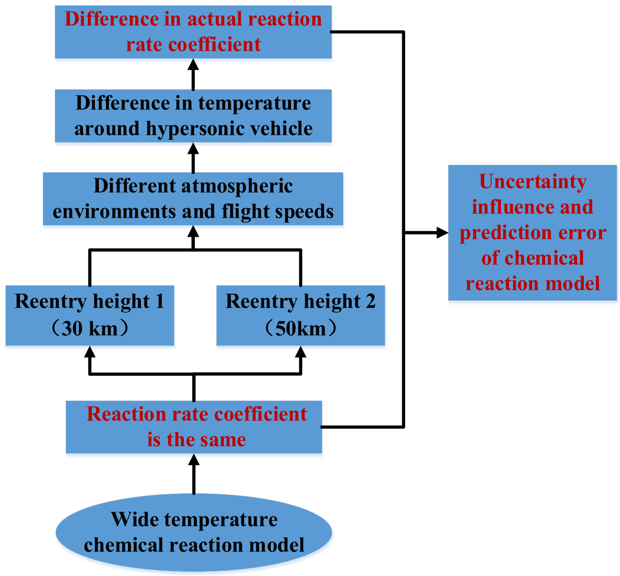

Fig. 1. Existence and analysis of uncertainty of chemical reaction model in different reentry height cases.

solver and FDTD method, and verified that high-power microwave can enhance the ability of low-frequency EM waves to pass through plasma sheath [15–16]. Ouyang *et al* have developed hypersonic plasma flow model under thermochemical non-equilibrium (7 species chemical model and two-temperature model) based on USim code, and proposed a new vehicle shape optimization scheme for mitigating RF blackout problem [17]. Obviously, hypersonic plasma flow model developed in the above work plays an important role in vehicle communication prediction and RF blackout mitigation schemes.

Chemical reaction models under hypersonic plasma flow are used to describe the chemical non-equilibrium effect, which almost adopts the model proposed by Park and Gupta [18–20]. These chemical models are suitable for a wide temperature range, but reaction coefficients of these models are determined by experimental results at specific temperature, which will lead to a certain uncertainty in the reaction coefficients of chemical model. In 2018, Jung *et al* have proposed the concept of uncertainty of chemical reaction rate model and analyzed its impact on plasma distribution and reentry communication attenuation, related results show that the impact of associated ionization reaction is most significant [21–22]. In 2020, Ouyang *et al* have further quantitatively studied the impact of ionization and non-ionization reaction rates on plasma sheath characteristics and communication attenuation, the influence of ionization reaction rate is much greater than that of non-ionization reaction [23–24]. In 2021, Takasawa *et al* have verified theoretically and experimentally that reducing the ionization reaction rate via surface catalysis can effectively reduce the electron density and electromagnetic wave attenuation [25–26].

Although the above studies have verified that the rate uncertainty of chemical model has a significant impact on the prediction of the plasma sheath and reentry communication, they all change the reaction rate through artificial or catalytic action to observe the impact of rate uncertainty. However, when wide temperature chemical reaction model applied to the research of different flight parameters or vehicle shapes, influence of uncertainty of reaction coefficient is really existing. As shown in Fig. 1, taking different reentry heights as an example, reaction coefficients of chemical model applied to different reentry heights are completely consistent. However, the atmospheric environment and vehicle speed at different reentry heights are completely different, which will lead to different temperatures around hypersonic vehicle [1,27–29]. Different temperatures will further lead to different actual reaction coefficients, so uncertainty of chemical reaction model will cause certain errors in the prediction of plasma sheath and communication attenuation at different reentry heights (It is also the same for different flight parameters and vehicle shapes). In addition to the detailed analysis of uncertainty effects of chemical reaction models under different reentry heights, how to reduce or even eliminate the errors caused by uncertainty effects of reaction rates also needs to be further studied.

This paper is organized as follows. In Sec. 2, OCR model considering the uncertainty of temperature reaction rate coefficient at different reentry heights is proposed, and the coupling of hypersonic plasma flow model and OCR model, and joint simulation process with terahertz transmission model are introduced in detail. In Sec. 3, phenomenon of reaction rate uncertainty under different re-entry heights, and influence of reaction rate uncertainty on the plasma sheath and terahertz transmission characteristics are analyzed and discussed. Finally, related conclusions are summarized in Sec. 4.

Description of model

The uncertainty of chemical reaction model coefficients caused by different temperatures around RAM C vehicle (Specific configuration of RAM C vehicle can be observed in reference [23]) in different reentry heights is first analyzed by hypersonic plasma flow model, which has been validated by flight test data in previous work [23–24]. Then, by considering the change of the actual reaction rate coefficient caused by temperature difference around vehicle at different reentry heights, the chemical reaction optimization model is developed to analyze the influence of reaction rate uncertainty under different flight conditions. Finally, by coupling the hypersonic plasma flow model and chemical reaction optimization model considering influence of uncertainty, the plasma sheath characteristics at different reentry heights are solved and compared with original plasma flow model results and flight data. Furthermore, reentry communication attenuation considering the influence of uncertainty of reaction rate coefficient under different reentry heights is discussed based on the SMM method.

Hypersonic plasma flow model

Hypersonic plasma flow model developed in previous is expressed by the Navier-Stokes (N-S) governing equations in two-dimensional form.

$$\frac{\partial \boldsymbol{Q}}{\partial t}+\frac{\partial \boldsymbol{F}}{\partial x}+\frac{\partial \boldsymbol{G}}{\partial y}=\frac{\partial \boldsymbol{F}_v}{\partial x}+\frac{\partial \boldsymbol{G}_v}{\partial y}+\boldsymbol{\omega} \tag{1}$$

where $\boldsymbol{Q}$ and $\boldsymbol{\omega}$ represent the conservative vector and source term, $\boldsymbol{F}$ and $\boldsymbol{F}_v$ refer to the convective flux vector at x and y directions, $\boldsymbol{G}$ and $\boldsymbol{G}_v$ refer to the viscous flux vector at x and y directions. The 7 species 18 chemical reaction model and single temperature model are used to describe the chemical non-equilibrium effects and thermodynamic equilibrium state in this paper, the seven species are N_2,O_2,NO,N,O,NO^+, e. Therefore, the N-S governing equations can be expanded as:

$$\boldsymbol{Q}=\begin{bmatrix}\rho\\ \rho u\\ \rho v\\ E\\ \rho_s\end{bmatrix},\boldsymbol{F}=\begin{bmatrix}\rho u\\ \rho u^2+p\\ \rho uv\\ (E+p)u\\ \rho_s u\end{bmatrix},\boldsymbol{G}=\begin{bmatrix}\rho v\\ \rho uv\\ \rho v^2+p\\ (E+p)v\\ \rho_s v\end{bmatrix} \tag{2}$$

$$\boldsymbol{F}_v=\begin{bmatrix}0\\ \tau_{xx}\\ \tau_{xy}\\ u\tau_{xx}+v\tau_{xy}+q_x+\rho_s H_{s,x}\\ J_{s,x}\end{bmatrix} \tag{3}$$

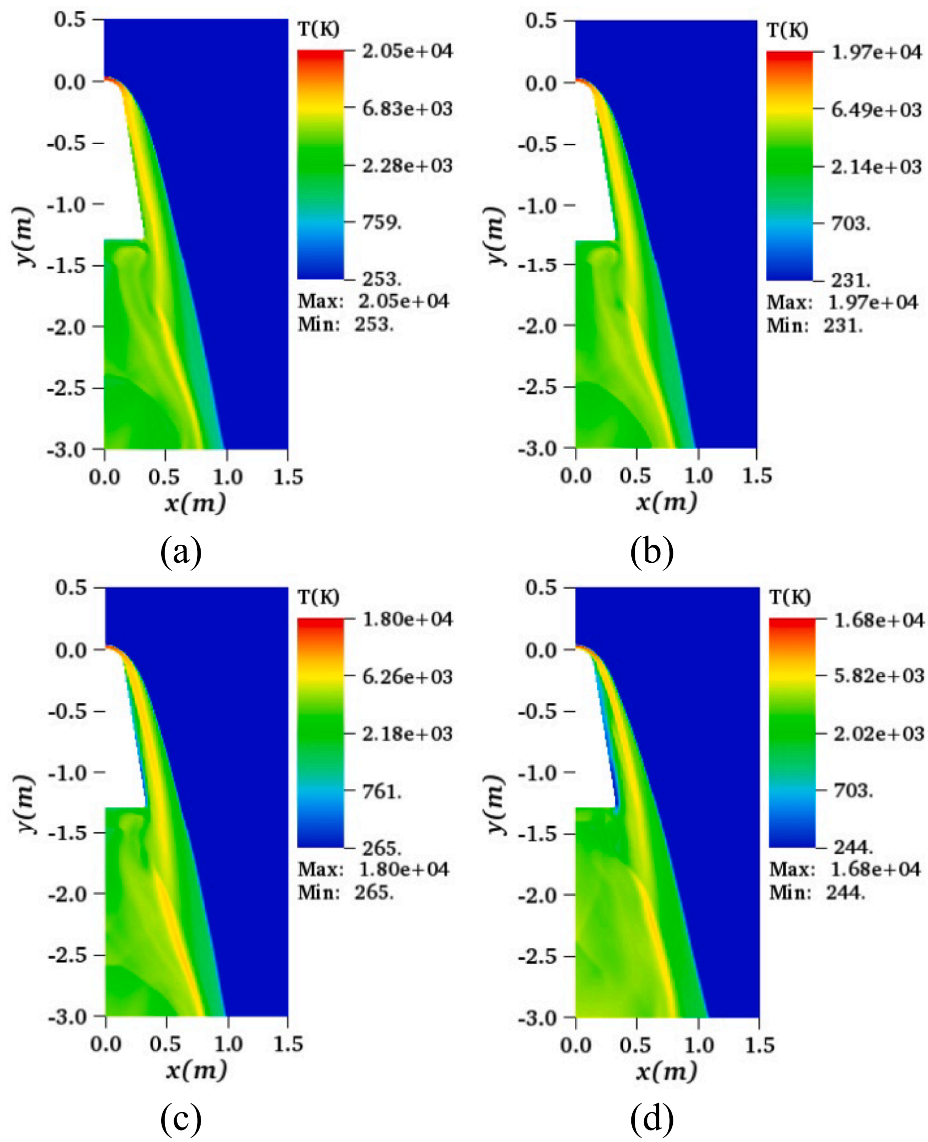

Fig. 2. Temperature distribution around RAM C vehicle under different reentry heights. (a) 30 km. (b) 40 km. (c) 50 km (d) 61 km.

$$\boldsymbol{G}_v = \begin{bmatrix} 0 \\ \tau_{yx} \\ \tau_{yy} \\ u\tau_{xy} + v\tau_{yy} + q_y + +\rho_s H_{s,x} \\ J_{s,y} \end{bmatrix}, \boldsymbol{\omega} = \begin{bmatrix} 0 \\ 0 \\ 0 \\ 0 \\ \dot{\omega}_s \end{bmatrix} \tag{4}$$

where ρ refer to the density, u and v represent the flow speed in the x and y directions. p and E represent the total pressure and energy, which can be obtained by thermodynamic model [23–27]. τ refer to the total pressure and stress tensor, q, H and J are the heat, enthalpy and diffusion flux, these parameters can be calculated by transport model [15–17]. $\dot{\omega}_s$ refer to the change rate of species density, which can be obtained by chemical nonequilibrium model [9–12].

Optimized chemical reaction model

For different reentry heights, the flight speed and atmospheric environment (initial temperature, pressure and density of freestream) all changed during vehicle reentry, as show in Table 1 [16]. The changes in flight parameters will cause the changes in temperature around vehicle, which will further affect the reaction rate of chemical reactions. In order to clarify that the current wide temperature chemical reaction model needs to be further optimized to reduce the influence of the uncertainty of reaction rate coefficient, the influence of reentry height on the temperature around vehicle is first analyzed.

Fig. 2 compares the temperature distribution under different reentry heights based on the hypersonic plasma flow model, the reentry height range considered in this work is 30 ~ 61 km, corresponding hypersonic vehicle is RAM C vehicle and the configuration parameters of RAM C vehicle can be found in reference [23–24]. Maximum temperatures around RAM C vehicle corresponding to the reentry heights of 30 km, 40 km, 50 km, and 61 km are 2.05×10^4 K, 1.97×10^4 K, 1.80×10^4 K and 1.68×10^4 K, respectively.

Although the temperature around vehicle cannot fully represent the temperature of actual chemical reaction, there is a positive correlation between the two. The higher the temperature around vehicle is, the higher the temperature of actual chemical reaction is. The increase of actual reaction temperature will inevitably lead to the increase of chemical reaction rate. Therefore, the wide temperature chemical reaction model should consider the effect of flight parameters on the reaction rate and be further optimized.

The specific chemical reactions and related reaction parameters of

Table 1
Initial conditions for different heights.

Height (km)	Temperature (K)	Density (kg/m^3)	Velocity (m/s)
30	231.2	1.801×10^{-2}	6550
40	253.2	4.360×10^{-3}	7380
50	266.2	1.150×10^{-3}	7620
61	244.3	2.816×10^{-4}	7650

Table 2
Related reaction coefficient of OCR model.

r	Chemical reaction	A	n'	E_a
1–3	$N_2 + M_1 \rightleftharpoons N + N + M_1$	$f_1 \times 6.76 \times 10^{-13}$	−1.6	9.41×10^5
4–5	$N_2 + M_2 \rightleftharpoons N + N + M_2$	$f_1 \times 2.01 \times 10^{-12}$	−1.6	9.41×10^5
6–8	$O_2 + M_1 \rightleftharpoons O + O + M_1$	$f_2 \times 1.53 \times 10^{-13}$	−1.0	4.95×10^5
9–10	$O_2 + M_2 \rightleftharpoons O + O + M_2$	$f_2 \times 4.60 \times 10^{-10}$	−1.0	4.95×10^5
11–13	$NO + M_1 \rightleftharpoons N + O + M_1$	$f_3 \times 3.82 \times 10^{-13}$	0.0	6.28×10^5
14–15	$NO + M_2 \rightleftharpoons N + O + M_2$	$f_4 \times 4.42 \times 10^{-14}$	−0.5	6.28×10^5
16	$N_2 + O \rightleftharpoons NO + N$	$f_5 \times 2.99 \times 10^{-17}$	−0.1	3.13×10^5
17	$NO + O \rightleftharpoons O_2 + N$	$f_6 \times 5.58 \times 10^{-19}$	1.29	1.60×10^5
18	$N + O \rightleftharpoons NO^+ + e$	$f_7 \times 1.08 \times 10^{-18}$	0.0	2.66×10^5

$M_1 = N_2, O_2, NO$; $M_2 = N, O$.

currently commonly used wide-temperature chemical reaction models (which is defined as the TCR model in this paper) are shown in Table 1 [9–12,17–20]. According to the relevant shock wave experiments, flight experiments and simulation results [18–20,22–23,30], actual reaction temperature T_{sr} corresponding to TCR model is set to be 20000 K in this paper. The electron density calculation results of current hypersonic plasma flow model are all higher than flight data [6–14], which indicates that the plasma sheath formation process considered in the plasma flow model is more violent than the experimental results. Therefore, the vehicle surface temperature T_{vr} of classic case of RAM C vehicle under reentry height of 30 km was considered to correspond to the reaction temperature of TCR model (Fig. 2(a)), which is equal to 20500 K.

$$T_{sr} = 20000K, T_{vr} = 20500K \tag{5}$$

It is no doubt that there is a positive correlation between the vehicle surface temperature and actual reaction temperature Therefore, it is considered in this paper that the temperature around vehicle is proportional to the actual temperature of chemical reaction.

$$\frac{T_{vr}}{T_{sr}} = \frac{T_{vr}{}^h}{T_{sr}{}^h} \tag{6}$$

where $T_{vr}{}^h$ and $T_{sr}{}^h$ represent the vehicle surface temperature and actual reaction temperature at different reentry heights, and $T_{vr}{}^h$ can be calculated by hypersonic plasma flow model (Fig. 2). Therefore, the actual reaction temperature at different reentry heights can be obtained according to equations (5) and (6).

The modified Arrhenius formula with four parameters is expressed as:

$$k_f(T) = A\left(\frac{T}{298}\right)^{n'} \exp\left(-\frac{E_a}{T}\right) \tag{7}$$

where n' represents an exponential constant, and the values of n' corresponding to different chemical reactions can be obtained from Table 2.

The forward reaction rate at a certain reentry height is expressed as:

$$k_f\left(T_{sr}{}^h\right) = A\left(\frac{T_{sr}{}^h}{298}\right)^{n'} \exp\left(-\frac{E_a}{T_{sr}{}^h}\right) \tag{8}$$

where A, n, and E_a are the forward rate constant coefficient, as show in Table 2. Combining Eqs. (6) and (8), we can get:

$$k_f\left(T_{sr}{}^h\right) = A\left(\frac{T_{sr}}{298}\right)^{n'}\left(\frac{T_{vr}{}^h}{T_{vr}}\right)^{n'} \exp\left(-\frac{E_a}{T_{sr}}\right) \times \exp\left(-\frac{E_a}{T_{sr}}\left(\frac{T_{vr}}{T_{vr}{}^h} - 1\right)\right) \tag{9}$$

The simplified transformation of Eq. (9) leads to:

$$k_f\left(T_{sr}{}^h\right) = k_f(T_{sr})\left(\frac{T_{vr}{}^h}{T_{vr}}\right)^{n'}\left(-\frac{E_a}{T_{sr}}\left(\frac{T_{vr}}{T_{vr}{}^h} - 1\right)\right)^{n'} \tag{10}$$

Therefore, the influence coefficient of chemical reaction uncertainty f at different reentry heights can be obtained according to Eq. (10).

$$f = \frac{k_f\left(T_{sr}{}^h\right)}{k_f(T_{sr})} = \left(\frac{T_{vr}{}^h}{T_{vr}}\right)^{n'}\left(-\frac{E_a}{T_{sr}}\left(\frac{T_{vr}}{T_{vr}{}^h} - 1\right)\right)^{n'} \tag{11}$$

It should be noted that the values of n' and E_a corresponding to different chemical reactions (such as $N + O \rightleftharpoons NO^+ + e$, $NO + N \rightleftharpoons N + O + N$, $N_2 + O_2 \rightleftharpoons N + N + O_2$, etc.) are different, which will lead to different values of the uncertainty influence coefficient f corresponding to different reactions in the chemical reaction model. Therefore, the uncertainty influence coefficients corresponding to chemical reactions 1–5, 6–10, 11–13, 14–15, 16, 17 and 18 are f_1 f_7, respectively, as show in Table 2. Therefore, chemical reaction model is optimized by compensating the uncertainty influence coefficient.

Terahertz wave propagation model in plasma sheath

EM wave attenuation in reentry plasma sheath is solved by SMM method [17,24], the principle of SMM method is to divide the plasma sheath into m uniform thin layers with a thickness of $\Delta d = d_m - d_{m-1}$. Each thin layer of plasma can be regarded as an electromagnetic loss medium, and the plasma relative permittivity can be obtained from the data of electron density and collision frequency solved by hypersonic plasma flow model coupled with OCR model.

$$\varepsilon_{r,n} = 1 - \frac{(w_p/v_e)^2}{1 + (w/v_e)^2} - j\frac{w_p{}^2/wv_e}{1 + (w/v_e)^2} \tag{12}$$

where w_p is plasma frequency, which is determined by electron density, v_e and w refer to the collision frequency and EM wave angular frequency. Subscript n is the number of plasma layers.

EM wave propagation characteristics through plasma sheath can be expressed in global matrix form.

$$S_g = \prod_{n=1}^{n=m} S_n = \begin{bmatrix} S_{g1} & S_{g2} \end{bmatrix} \tag{13}$$

where S_m can be calculated as:

$$S_m = \begin{bmatrix} 1 & 1 \\ k_m & -k_m \end{bmatrix}^{-1} \begin{bmatrix} e^{-Q_{m-1}} & e^{Q_{m-1}} \\ k_{m-1}e^{-Q_{m-1}} & -k_{m-1}e^{Q_{m-1}} \end{bmatrix} \tag{14}$$

where Q_{m-1} can be solved as:

$$Q_{m-1} = jk_{m-1}\Delta d \tag{15}$$

where k refers to the wavenumber, which can be calculated as:

$$k_m = k_0\sqrt{\varepsilon_{r,m}} \tag{16}$$

where k_0 refers to the wavenumber of free space, which can be solved by $k_0 = 2\pi f_0/c$. f_0 and c represent the EM wave frequency and speed of light, respectively.

Through the electromagnetic boundary matching between different plasma layers, the transmission T and reflection R coefficients of EM waves can be solved by the global matrix.

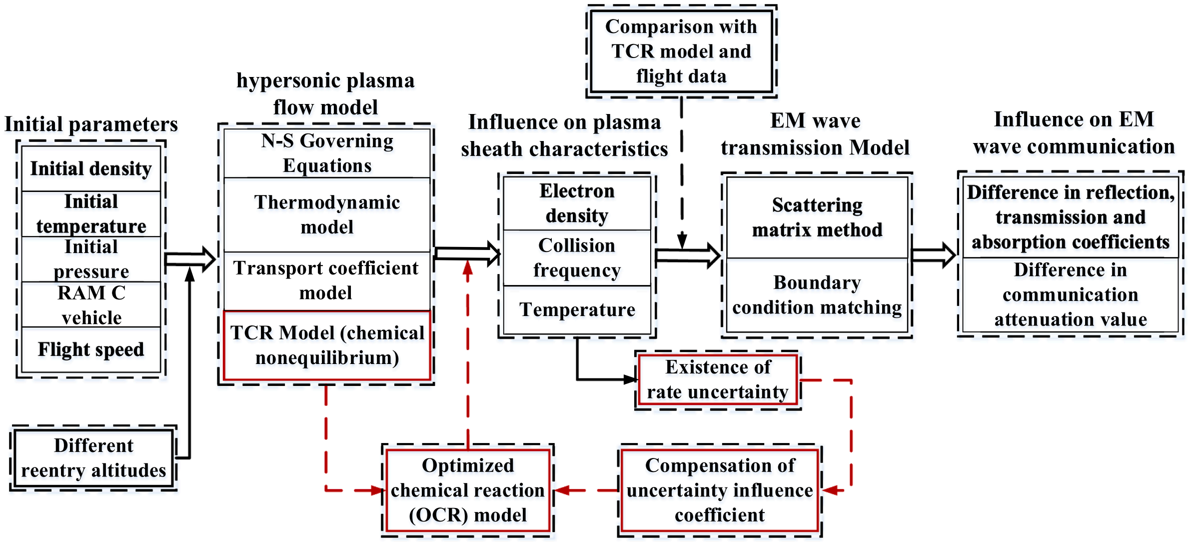

Fig. 3. Joint simulation process of hypersonic plasma flow model coupled with OCR model and EM wave transmission model.

$$\begin{bmatrix} R \\ T \end{bmatrix} = -[S_{g2} \quad -V]^{-1} \cdot S_{g1} \tag{17}$$

where V can be obtained as:

$$V = \frac{1}{2k_m} \begin{bmatrix} (k_m + k_{m+1})e^{Q_m} \\ (k_m - k_{m+1})e^{-Q_m} \end{bmatrix} \tag{18}$$

According to the transmission coefficient and reflection coefficient of EM wave, the absorption coefficient A can be solved.

$$|A|^2 = 1 - |R|^2 - |T|^2 \tag{19}$$

The power transmission T_p, power reflection R_p and power absorption A_p coefficients are expressed as:

$$T_p = |T|^2, R_p = |R|^2, A_p = 1 - T_p - R_p \tag{20}$$

Finally, the specific attenuation value G (in dB) of EM wave passing through the plasma sheath can be calculated according to the transmission coefficient.

$$G = 20lg|T| \tag{21}$$

Joint simulation process of multi-physical field model

Based on the hypersonic plasma flow model, OCR model and EM wave transmission model, a joint simulation model is developed to investigate the influence of uncertainty of chemical reaction model on the plasma sheath and terahertz transmission characteristics under different reentry heights, and verify the accuracy of the prediction results of OCR model by compensating the uncertainty influence coefficient. The specific joint simulation process as shown in Fig. 3.

Firstly, the surface temperature around RAM C vehicle is solved by hypersonic plasma flow model, the difference in reaction rate coefficient caused by different temperatures is analyzed, and the existence of uncertainty of reaction coefficient at different reentry heights is determined. Secondly, by coupling the hypersonic plasma flow model and the OCR model considering the uncertainty of feedback reaction coefficient, plasma sheath characteristics under different reentry heights are solved and compared with TCR model results and flight data. Finally, based on the above plasma sheath distribution solved, the EM wave transmission characteristics at different reentry heights considering the influence of the uncertainty of reaction coefficient are further analyzed, and compared with the results under TCR model.

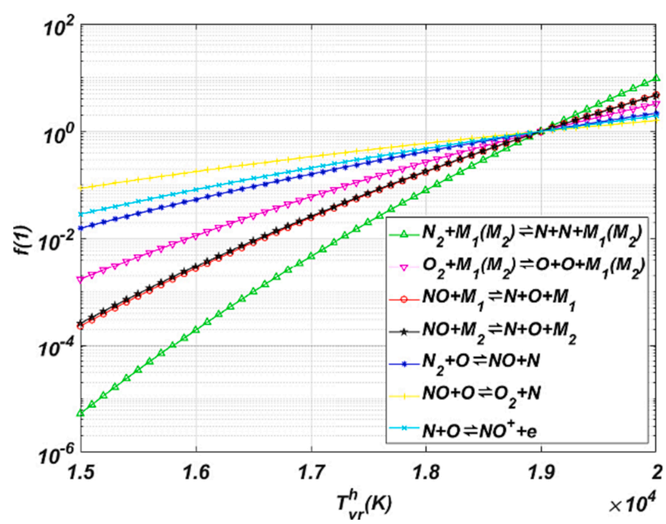

Fig. 4. Relationship between the rate uncertainty influence coefficient and temperature around vehicle at different reentry heights.

Results and discussion

Analysis of influence coefficient of reaction rate uncertainty under different reentry heights

In Section 2.2, it has been determined that the temperature difference at different reentry heights will lead to the uncertainty of the reaction rate coefficient by analyzing the temperature around vehicle at 30 ~ 61 km (Fig. 2), and a model for the influence coefficient of reaction rate uncertainty has been derived (Equation (11)). Based on the calculation equation of influence coefficient of reaction rate uncertainty, the relationship between the temperature around vehicle and influence coefficient of reaction rate uncertainty is solved. As shown in Fig. 4, the reaction rate coefficient corresponding to different temperatures around the vehicle are completely different.

According to Fig. 4, with the increase of temperature, rate uncertainty influence coefficient of chemical reaction all increases, which means the increasing of reaction rate, but different chemical reactions show differential responses to temperature around vehicle. Temperature has the most significant effect on the reaction rate uncertainty

Table 3
Correction of chemical reaction coefficients under different reentry heights.

Reentry height	f_1	f_2	f_3	f_4	f_5	f_6	f_7
30 km	1.0	1.0	1.0	1.0	1.0	1.0	1.0
40 km	0.08	0.27	0.17	0.18	0.42	0.60	0.48
50 km	0.02	0.11	0.06	0.06	0.24	0.43	0.29
61 km	0.01	0.04	0.02	0.02	0.13	0.30	0.18

coefficient of $N_2 \rightleftharpoons N+N$ (reactions 1–5) and $NO \rightleftharpoons N+O$ (reactions 11–15), the reaction rates of $NO+O \rightleftharpoons O_2+N$ (reaction (17) and $N+O \rightleftharpoons NO^+ +e$ (reaction (18) are relatively less affected. It is worth noting that although the rate uncertainty coefficient of ionization reaction is relatively less affected by temperature, the reaction rate increases by about 68 times when the temperature around vehicle increases from 15000 K to 20000 K. According to previous research results, the ionization reaction has the most significant effect on the electron density in all chemical reactions, changes in the ionization rate by several tens of times affect the electron density by more than an order of magnitude [22–26]. Therefore, the uncertainty of reaction rate at different reentry heights actually exists, and it will obviously have a certain impact on the characteristics of the plasma sheath.

Based on the temperature around vehicle in Fig. 2 and the influence coefficient of reaction rate uncertainty are solved by Equation (11), as shown in Table 3. It is obvious that the reaction rates of various chemical reactions have changed to varying degrees with the change of reentry height. The influence of reaction coefficient uncertainty under different heights on the plasma sheath and EM wave transmission characteristics will be further discussed in the next section.

Impact of chemical reaction uncertainty under different heights on the plasma sheath characteristics

Based on the coupling of OCR model considering reaction rate uncertainty and hypersonic plasma flow model, the plasma sheath characteristics under different reentry heights are numerically solved. Fig. 5 shows the electron density distribution calculated by OCR model under different reentry heights. It is obvious that compared with TCR model, the electron density predicted by OCR model considering reaction rate uncertainty under different reentry heights decreases slightly. The peak electron density reduced from 1.70×10^{21} to 1.59×10^{21} m^{-3} under 40 km, reduced from 5.30×10^{20} to 4.47×10^{20} m^{-3} under 50 km, and reduced from 1.27×10^{20} to 7.76×10^{19} m^{-3} under 61 km. The reason is that the influence coefficient of rate uncertainty is compensated under OCR model and the chemical reaction rate significantly reduces, especially the reduction of ionization reaction rate (reaction (17) leads to the reduction of electron density.

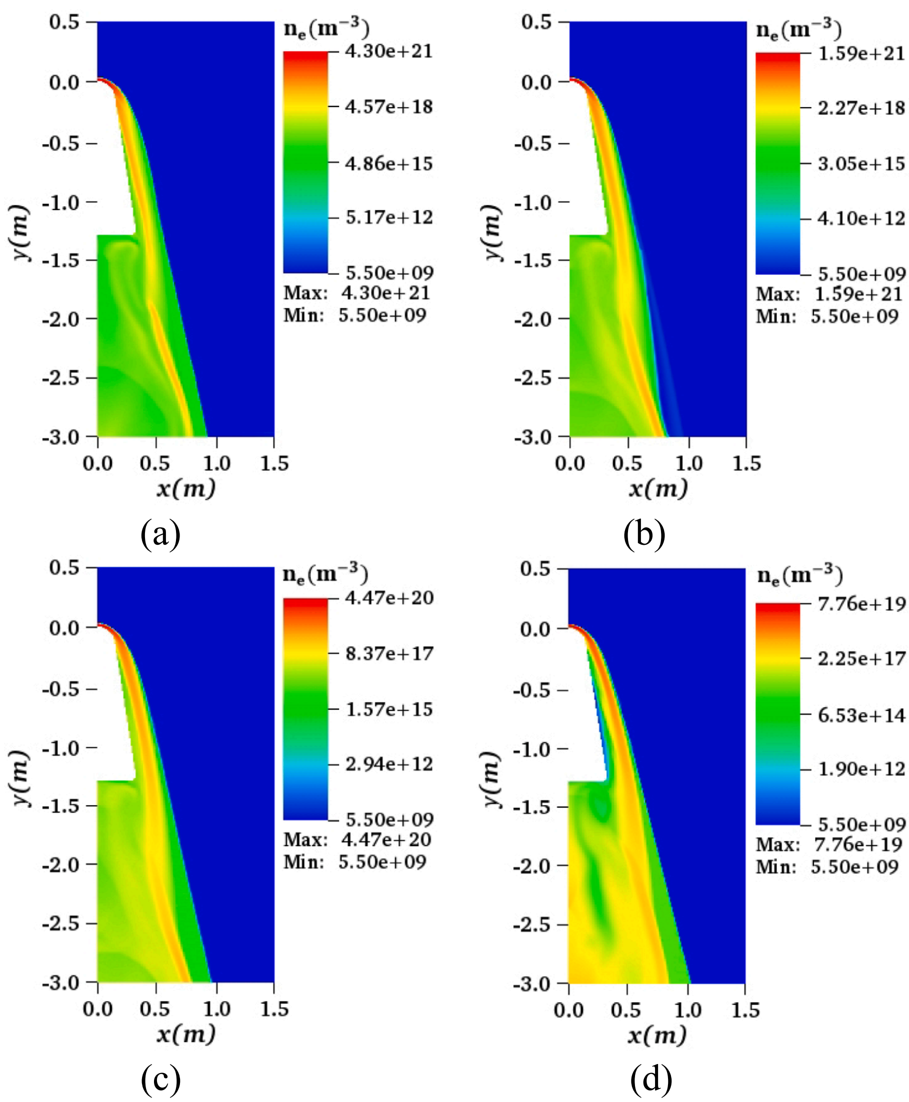

Fig. 5. Electron Density distribution around RAM C vehicle based on the OCR model under different reentry heights. (a) 30 km. (b) 40 km. (c) 50 km (d) 61 km.

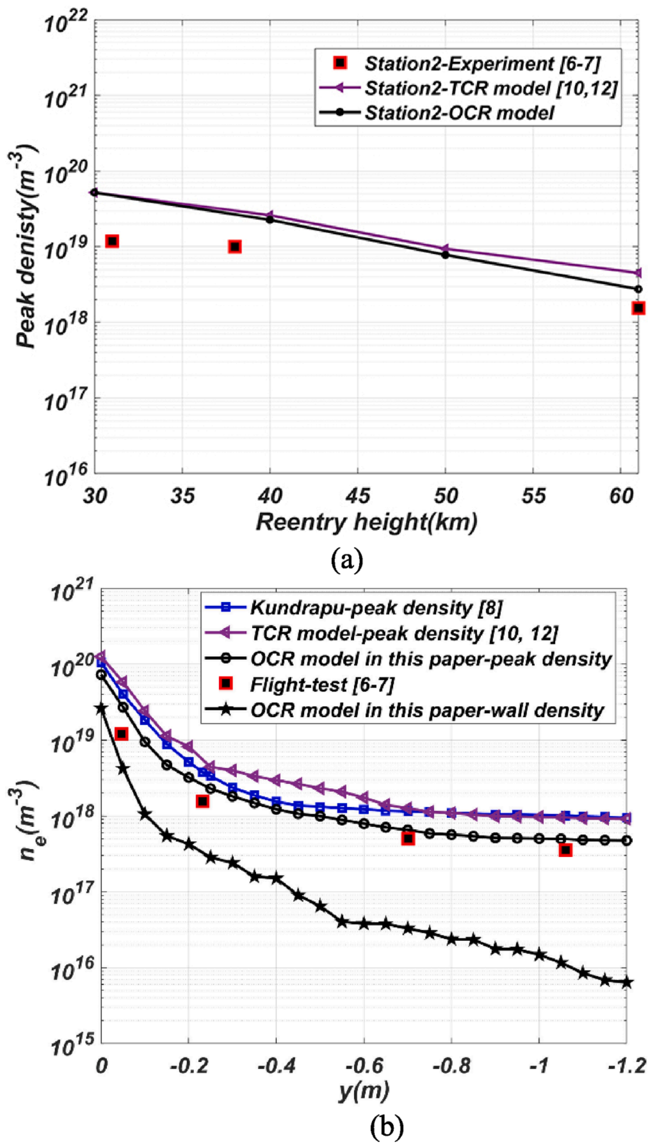

Fig. 6. Comparison of electron density of the OCR model with the TCR model and flight test experiments. (a) Different reentry heights at station 2. (b) Different stations at 61 km.

In order to further verify the prediction results based on the OCR model, Fig. 6 compares the peak electron density under different reentry heights and stations with that of TCR model and flight experiments. In the flight tests of RAM C vehicle, a number of microwave reflectometers were installed at four stations (y = -0.046 m, −0.232 m, −0.701 m and −1.060 m) on the vehicle surface to measure the electron density in reentry plasma sheath.

It is obvious from Fig. 6 that the variation trend of electron density under OCR model and TCR model are all in good agreement with the flight experiment data at different reentry heights and stations. However, the electron density of OCR model has less error than that of TCR model compared with the flight experiment data, especially at the reentry altitude of 61 km (Fig. 6(a)). The electron density corresponding to OCR model and TCR model under 40 km are 2.60×10^{19} m^{-3} and 2.26×10^{19} m^{-3}, respectively. Prediction accuracy for electron density of OCR model is improved by about 13.1%. The electron density corresponding to OCR model and TCR model under 61 km are 2.65×10^{18} m^{-3} and 4.50×10^{18} m^{-3}, respectively. Prediction accuracy for electron density of OCR model is improved by about 38.9%. The reason for the significant improvement in prediction accuracy is that the corrected ionization reaction coefficient of OCR model under 61 km is about 0.18 times that of traditional wide-temperature TCR model, resulting in a closer electron density to the measurement results of flight data.

In addition, the electron density for different antenna stations at 61 km of OCR model were compared with other researchers and flight experiment data (Fig. 6(b)). The calculated electron densities of TCR under the plasma flow model are in good agreement with other researchers' results, which have also been reported in previous studies [8,10,12]. It is worth noting that no matter where the antenna station is, the electron density of the OCR model proposed in this paper is slightly lower than that of TCR model, and it is more consistent with the flight experiments.

According to the previous research results [8–12,27–29], electron density, collision frequency, and plasma sheath thickness are the main factors affecting the vehicle communication in the plasma sheath. Therefore, the effect of OCR model on the collision frequency was further analyzed, and the effect of plasma sheath thickness can be obtained from the electron density and collision frequency distribution. The electron collision frequency can be calculated according to pressure and temperature [31].

$$\nu_e = 5.814 \times 10^{12} \frac{p}{p_0} T^{-1/2} \tag{22}$$

where p_0 refers to the standard atmospheric pressure under different reentry heights.

Fig. 7 shows the collision frequency distribution under OCR model under different reentry heights. The peak collision frequencies corresponding to 30 km, 40 km, 50 km, and 61 km are 361 GHz, 114 GHz, 36.5 GHz and 13.4 GHz, respectively, which are consistent with the peak collision frequency values corresponding to wide temperature TCR model [8–12]. Furthermore, it is obviously that there is little difference in the collision frequency distribution and plasma sheath thickness between the OCR and TCR models. The reason is that the reaction rate correction considering influence of flight parameters feeds back the reaction rate through the temperature difference under different flight parameters, which has no effect on the original reaction temperature and pressure. Therefore, the collision frequency and plasma sheath thickness are not affected by the reaction rate uncertainty, which is in full agreement with Ref. [10].

Fig. 8 further compare the specific distribution of electron density on the terahertz wave transmission path under TCR model with OCR model considering the influence of reaction rate uncertainty. The collision frequency is not affected by the reaction rate uncertainty, which is in full agreement with Ref. [10]. The terahertz wave antenna is located at y = -0.6 m on the vehicle surface. Obviously, except for the reentry altitude of 30 km, the electron density of the OCR model at 40 ~ 61 km along the terahertz transmission path has a certain degree of decline. The reason is that when discussing the influence of uncertain reaction speed caused by temperature differences at different re-entry altitudes, in this paper, the temperature at a re-entry altitude of 30 km (the highest temperature at all re-entry altitudes) is set to match the actual reaction temperature of the TCR model. And as the re-entry height increases, the electron density of OCR model decreases more than that of the TCR model. The maximum electron density on the terahertz transmission path decreases from 2.24×10^{19} m^{-3} to 1.95×10^{19} m^{-3} (0.87 times) at 40 km, decreases from 7.8×10^{18} m^{-3} to 5.55×10^{18} m^{-3} (0.71 times) at 50 km, decreases from 5.94×10^{18} m^{-3} to 3.34×10^{18} m^{-3} (0.56 times) at 61 km.

Based on the above analysis, the influence of reaction rate uncertainty under different reentry heights on the plasma sheath characteristics is mainly concentrated on the influence of electron density, and has little effect on the collision frequency and the sheath thickness. And because the re-entry altitude of 30 km is set to correspond to the reaction temperature of TCR model, the electron density data of OCR and TCR at 30 km are also consistent. Therefore, the influence of reaction rate

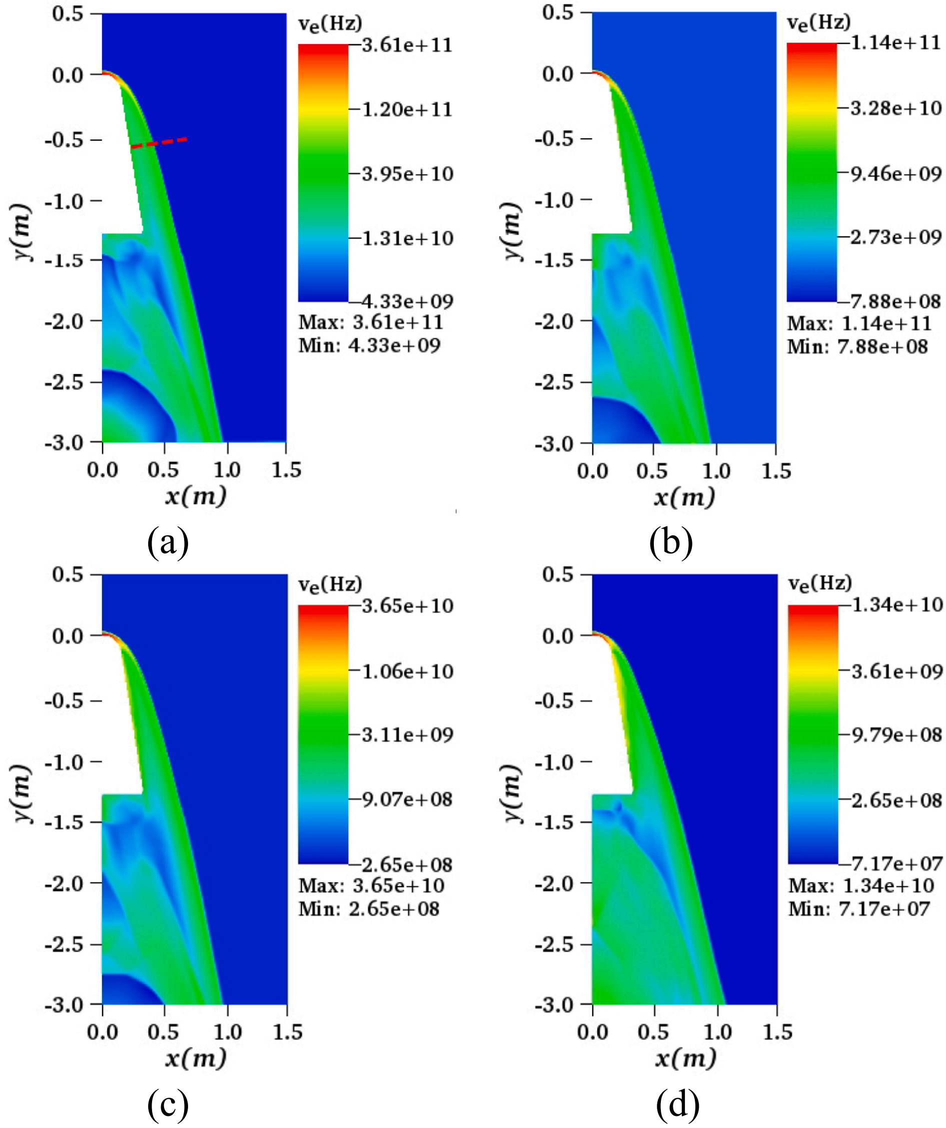

Fig. 7. Collision frequency distribution around RAM C vehicle based on the OCR model under different reentry heights. (a) 30 km. (b) 40 km. (c) 50 km (d) 61 km.

uncertainty on the terahertz transmission characteristics under different re-entry heights will be further discussed in the next section based on the influence analysis of plasma sheath characteristics, and the re-entry heights of 40 km, 50 km, 61 km are focused on.

Impact of chemical reaction uncertainty under different heights on the terahertz wave transmission characteristics

The peak electron density range on the 40 ~ 61 km of TCR model and OCR model is from 3.34×10^{18} m^{-3} to 2.24×10^{19} m^{-3}, and the corresponding plasma frequency is 16.2 ~ 42 GHz. Considering the thickness of reentry plasma sheath, EM wave frequencies used in this paper for vehicle communication are set to 0.05 ~ 0.5 THz, which belongs to sub-terahertz and terahertz bands. Fig. 9 compares the power absorption, reflection, transmission coefficients and signal attenuation of terahertz wave under TCR model and OCR model.

It is obvious from Fig. 9 that the variation trend of terahertz absorption, reflection, transmission and attenuation with the terahertz frequency and reentry height under OCR model is completely consistent with the TCR model. As the terahertz frequency increases, the transmission coefficient increases and leads to a decrease in signal attenuation, and the absorption coefficient and the reflection coefficient are reduced. As the increases of re-entry height, the electron density on the terahertz wave transmission path gradually decreases (Fig. 8), resulting in an increase in terahertz wave transmission coefficient, and decrease in signal attenuation, absorption coefficient, and reflection coefficient. In addition, the power absorption coefficient of terahertz waves varies inversely with the transmission coefficient, and the reflection coefficient is less than 0.01 in any terahertz wave band and re-entry height. Therefore, the terahertz attenuation under RAM C vehicle is mainly determined by the absorption effect, and contribution of the reflection effect to terahertz wave attenuation is almost negligible, the contribution mechanism of terahertz wave attenuation is exactly the same as that observed in the OCR model and TCR model.

However, regardless of any terahertz wave frequency or reentry height, OCR model has higher power transmission coefficient, and lower reflection coefficient, absorption coefficient, signal attenuation than that of TCR model. The reason is that compared with TCR model, the OCR model takes into account the influence of uncertainty of the reaction rate, resulting in a lower electron density (Fig. 8), which fits better with the flight experiment data (Fig. 6). As the terahertz wave increases, the difference between the OCR model and TCR model becomes smaller. When the EM wave is in the sub-terahertz band and the frequency is 0.05 THz, the signal attenuation of TCR model and OCR model are −44.9 dB

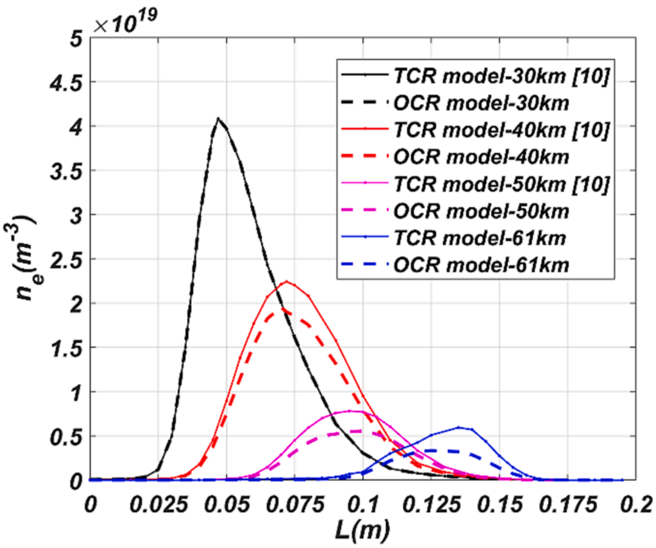

Fig. 8. Comparison of electron density of the TCR model with the OCR model on the terahertz wave transmission path. $L(m)$ represents the distance from the vehicle surface.

and −34.7 dB at 40 km, −20.5 dB and −15.4 dB at 50 km, and −9.0 dB and −6.6 dB at 61 km. At this time, the errors of OCR model and TCR model in the signal attenuation prediction results at 40 km, 50 km and 61 km are 22.7%, 24.9% and 26.7%, respectively. As the EM frequency continues to increase to 0.1 THz, the signal attenuation of TCR model and OCR model are −7.9 dB and −6.7 dB at 40 km, −5.1 dB and −4.2 dB at 50 km, and −2.3 dB and −1.8 dB at 61 km, and the errors of OCR model and TCR model in the signal attenuation prediction results at 40 km, 50 km and 61 km are reduced to 15.2%, 17.6% and 21.7%, respectively.

Compared with the traditional wide temperature TCR model, the OCR model considers the influence of flight parameters under different reentry heights on the chemical reaction rate coefficient and compensates the reaction rate uncertainty influence coefficient. The electron density prediction results show that OCR model developed in this paper is more consistent with the flight experiment data than the TCR model, and further leads to a difference of about 20% in the prediction results of terahertz attenuation compared with TCR model. Moreover, the critical communication frequencies of EM waves at 40 km, 50 km, and 61 km under OCR mode are 0.115 THz, 0.085 THz and 0.058 THz, respectively, which are about 0.01 THz lower than the critical communication frequency results obtained by the traditional TCR model.

Conclusions

An optimized chemical reaction model considering the uncertainty of reaction rate coefficient due to the temperature difference under different reentry altitudes is developed in this paper, and joint simulation with hypersonic plasma flow model and terahertz transmission model to study the influence of reaction rate uncertainty under different re-entry heights on the characteristics of plasma sheath and terahertz transmission.

Firstly, based on the OCR model, the influence of different vehicle surface temperatures on the uncertainty coefficient of chemical reaction

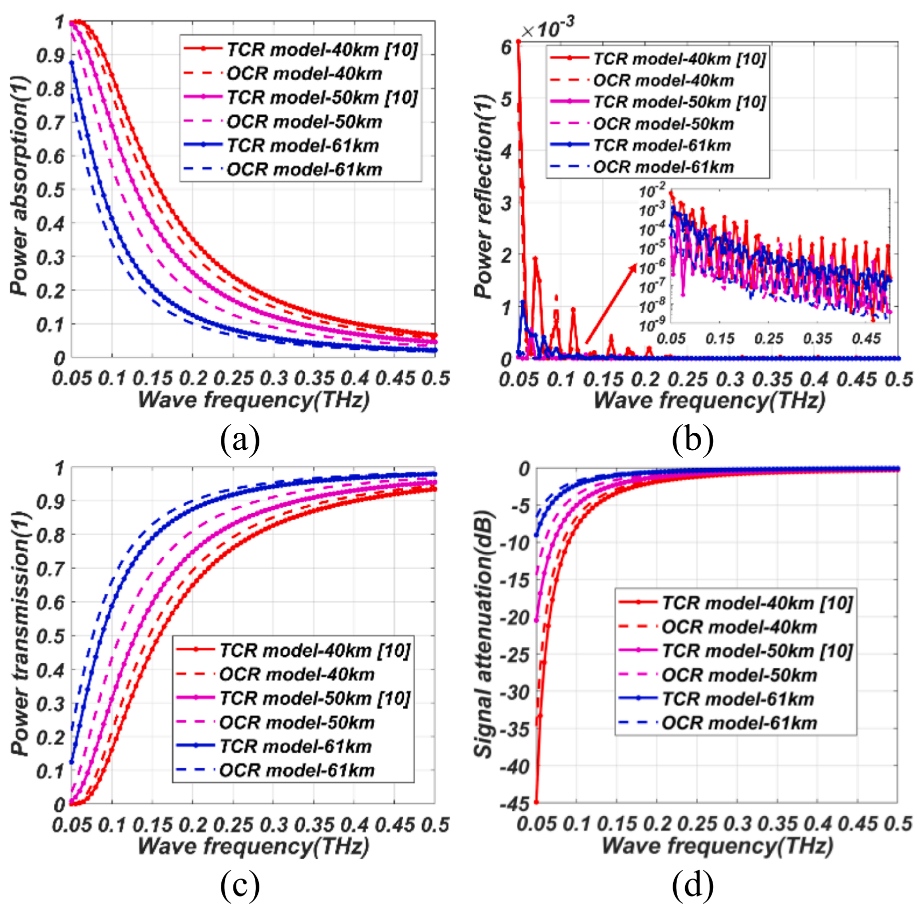

Fig. 9. Comparison of power absorption (a), reflection (b), transmission coefficients (c) and signal attenuation (d) of terahertz wave in wave transmission path under TCR model and OCR model.

rate is analyzed, and the specific value of reaction rate uncertainty coefficient is determined according to the vehicle surface temperature under different reentry altitudes. Then, the plasma sheath characteristics under different re-entry heights were solved by coupling the hypersonic plasma flow model with the reaction rate uncertainty coefficient obtained by OCR model. The reaction rate uncertainty mainly has a significant effect on the electron density, and has little effect on the collision frequency and sheath thickness. In addition, compared with the TCR model, the electron density results of OCR model are significantly closer to the flight data. Furthermore, the influence of reaction rate uncertainty on the transmission characteristics of terahertz waves is discussed through joint simulation with terahertz transmission model.

Although the changing trend of transmission, reflection, absorption coefficients and signal attenuation in the OCR model with re-entry height and terahertz frequency, and contribution mechanism of terahertz attenuation are completely consistent with TCR model, the prediction accuracy of signal attenuation at 0.05 THz improves about 25% than that of the TCR model, and error between the OCR model and the TCR model will gradually decrease with the increases of terahertz wave frequency. The OCR model developed in this paper is suitable for the research on the influence of flight speed, attitude angle of attack, atmospheric environment and other parameters on vehicle communication [9–12,28–29] and communication blackout scheme [21–26]. Since the OCR model can obtain a more accurate plasma sheath distribution, the relevant conclusions in the above-mentioned studies can be optimized, which is of great significance for the prediction of vehicle reentry communication and proposal of related communication schemes.

CRediT authorship contribution statement

Wenchong Ouyang: Data curation, Investigation, Writing – original draft, Writing – review & editing. **Chengbiao Ding:** Writing – review & editing, Formal analysis. **Qi Liu:** Writing – review & editing. **Quanming Lu:** Supervision. **Zhengwei Wu:** Conceptualization, Supervision, Funding acquisition, Project administration.

Declaration of Competing Interest

The authors declare that they have no known competing financial interests or personal relationships that could have appeared to influence the work reported in this paper.

Data availability

Data will be made available on request.

Acknowledgments

The authors would like to thank the anonymous reviewers and editors for their valuable comments and suggestions to improve the quality of this paper.

This work was supported in part by the ITER Project of the Ministry of Science and Technology under Grant No. 2022YFE03080001, supported by the joint Laboratory of Plasma Application Technology Funding, under Grant No. JL06120001H, and supported by the Fundamental Research Funds for the Central Universities No. USTC 20210079.

References

[1] Chen K, Xu DG, Li JN, et al. Studies on the propagation properties of THz wave in inhomogeneous dusty plasma sheath considering scattering process. Results Phys 2021;24:104109.
[2] Sha YX, Zhang HL, Guo XY, et al. Analyses of electromagnetic properties of a hypersonic object with plasma sheath. IEEE Trans Antennas Propag 2019;67(4):2470–81.
[3] Li CL, Liu DW, Liu B, et al. Chang'E-4 initial spectroscopic identification of lunar far-side mantle-derived materials. Nature 2019;5699(7756):378-+.
[4] Ding Y, Bai BW, Gao HJ, et al. An analysis of radar detection on a plasma sheath covered reentry target. IEEE Trans Aerosp Electron Syst 2021;57(6):4255–68.
[5] Sun SB, Liu S, Zhong SY. Analysis of terahertz wave penetration capacity to 2D conductive cylinder coated with steady-state parabolic distribution plasma media. Results Phys 2021;27:104516.
[6] Grantham WL. Flight results of a 25000-foot-per-second reentry experiment using microwave reflectometers to measure plasma electron density and standoff distance. NASA TN D-6062, Tech. Rep., Washington, D. C, 1970.
[7] Swift CT, Beck FB, Thomson J, et al. RAM C-III S-Band Diagnostic Experiment. NASA Special Publication 1971;253:137–55.
[8] Kundrapu M, Loverich J, Beckwith K, et al. Modeling radio communication blackout and blackout mitigation in hypersonic vehicles. J Spacecr Rockets 2015;52(3):853–62.
[9] Tang RX, Xiong ZF, Yuan K, et al. EHF Wave Propagation in the Plasma Sheath Enveloping Sharp-Coned Hypersonic Vehicle. IEEE Antennas Wirel Propag Lett 2021;20(6):978–82.
[10] Ouyang WC, Jin T, Wu ZW, et al. Study of terahertz wave propagation in realistic plasma sheath for the whole reentry process. IEEE Trans Plasma Sci 2021;49(1):460–5.
[11] Yuan K, Wang YH, Shen LF, et al. Sub-THz signals' propagation model in hypersonic plasma sheath under different atmospheric conditions. Science China Inf Sci 2017;60(11):113301.
[12] Ouyang WC, Deng WF, Wu ZW. Impact of Half-Angles on the Transmission of Terahertz Wave in Inhomogeneous Plasma Sheath. IEEE Trans Plasma Sci 2020;48(11):4029–36.
[13] Takahashi Y. Advanced validation of CFD-FDTD combined method using highly applicable solver for reentry blackout prediction. J Phys D Appl Phys 2016;49(1):015201.
[14] Takahashi Y. Propagation path of radio waves in nonequilibrium reentry plasma around a nanosatellite with an inflatable aeroshell. IEEE Trans Aerosp Electron Syst 2022;58(5):4070–82.
[15] Li J, He M, Li X, et al. Multiphysics modeling of electromagnetic wave-hypersonic vehicle interactions under high-power microwave illumination: 2-D case. IEEE Trans Antennas Propag 2018;66(7):3653–64.
[16] Wang KJ, Li J. Analyses of multiphysical model of electromagnetic and fluid in thermodynamic equilibrium and chemical nonequilibrium state. IEEE Trans Microw Theory Tech 2021;69(12):5228–40.
[17] Ouyang WC, Liu Q, Wu ZW. Difference analysis in the terahertz wave propagation in thermochemical nonequilibrium plasma sheath under different hypersonic vehicle shapes. Chin J Aeronaut 2022. https://doi.org/10.1016/j.cja.2023.07.001.
[18] Park C. Assessment of a two-temperature kinetic model for dissociating and weakly ionizing nitrogen. J Thermophys Heat Transfer 1988;2(1):8–16.
[19] Park C. Rotational relaxation of N2 behind a strong shock wave. J Thermophys Heat Transfer 2004;18(4):527–33.
[20] Gupta R N, Yos J M, Thompson R A, et al. A Review of Reaction Rates and Thermodynamic and Transport Properties for an 11 Species Air Model for Chemical and Thermal Nonequilibrium Calculations to 30000 K. NASA. Technical Report RP-1232, 1990.
[21] Jung M, Kihara H, Abe K, et al. Numerical simulation of plasma flows and radio-frequency blackout in atmospheric reentry demonstrator mission. AIAA Paper 2017::3308.
[22] Jung M, Kihara H, Abe KI, et al. Reentry blackout prediction for atmospheric reentry demonstrator mission considering uncertainty in chemical reaction rate model. Phys Plasmas 2018;25(1):013507.
[23] Ouyang WC, Liu YM. Impact of ionization rate on the transmission of electromagnetic wave in realistic plasma. Phys Plasmas 2020;27(3):033507.
[24] Ouyang WC, Liu Q, Zhang Z, Jin T, Wu ZW. Effect of non-ionizing reaction rate (assumed to be controllable) on the plasma generation mechanism and communication around RAMC vehicle during atmospheric reentry. Sci Rep 2021;11:20046.
[25] Takahashi Y, Enoki N, Takasawa H. Surface catalysis effects on mitigation of radio frequency blackout in orbital reentry. J Phys D Appl Phys 2020;53(3):235203.
[26] Takasawa H, Takahashi Y, Oshima N, et al. Experimental demonstration and mechanism of mitigating reentry blackout via surface catalysis effects. J Phys D Appl Phys 2021;54(22):225201.
[27] Ouyang WC, Liu YM, Deng WF, et al. Study of the electromagnetic wave propagation in realistic plasma. Microw Opt Technol Lett 2020;62(2):660–8.
[28] Yuan K, Chen JM, Shen LF, et al. Impact of reentry speed on the transmission of obliquely incident THz waves in realistic plasma sheaths. IEEE Trans Plasma Sci 2018;46(2):373–8.
[29] Yang X, Wei B, Yin WK. Relationship between the velocity of hypersonic vehicles and the transmission efficiency of radio waves. Waves Random Complex Media 2019;29(2):382–91.
[30] Boyda ID. Modeling of associative ionization reactions in hypersonic rarefied flows. Phys Fluids 2007;19(9):096102.
[31] Lankford D W. A study of electron collision frequency in air mixtures and turbulent boundary. Document No. AFWL-TR-72-71 (DTIC), 1972.